Applied Thermal Engineering 52 (2013) 420–427

Contents lists available at SciVerse ScienceDirect

Applied Thermal Engineering

journal homepage: www.elsevier.com/locate/apthermeng

Auto-ignition and combustion of diesel spray using unsteady laminar flamelet model

Isares Dhuchakallaya [a,*], Phadungsak Rattanadecho [a], Paul Watkins [b]

[a] Department of Mechanical Engineering, Thammasat University, Klong-Luang, Pathumthani 12120, Thailand
[b] School of Mechanical, Aerospace and Civil Engineering, University of Manchester, M13 9PL, UK

HIGHLIGHTS

- This model is able to capture the main features of the diesel flame structure.
- The flame shapes obtained are closely related to the luminous flames.
- The present model is apparently able to match the experimental results.
- The lifted flame is well represented by this developed model.

ARTICLE INFO

Article history:
Received 29 June 2012
Accepted 18 December 2012
Available online 2 January 2013

Keywords:
Auto-ignition
Combustion
Flamelet
Modelling
Spray

ABSTRACT

This work emphasises the modelling capabilities of the unsteady flamelet/reaction progress variable approach to implement diesel spray flames for capturing the auto-ignition and flame lift-off phenomena. The droplet size distribution based on the moment scheme characterises the poly-disperse spray model [1] employed in this work. The flamelet progress variable solutions embedded in a Reynolds-averaged Navier–Stokes (RANS) framework, together with the probability density function (PDF) approach, signify the turbulence–chemistry interaction. All thermochemical scalars are represented as a function of mean mixture fraction, mixture fraction variance, reaction progress variable and scalar dissipation rate. Mixture fraction is assumed to follow a beta-PDF distribution, because the reaction progress variable and scalar dissipation rate distributions are assumed to be a delta-PDF. In order to assess the capability of this developed model, the predicted results are compared with experimental data [2]. The developed model gives a reasonably good overall prediction performance in terms of auto-ignition, flame development and flame lift-off length. The flame temperature distributions are comparable with the formations of luminous flames. The predicted flame growth rate is consistent with the experimental results but there is a small over-prediction. Therefore, the present approach can accurately and efficiently capture the auto-ignition and flame lift-off phenomena of diesel spray flame.

1. Introduction

Due to superior fuel economy, spray combustion is utilised in a wide range of engineering devices, such as gas turbine engines and internal combustion engines. Because the fuel is injected into the high-temperature chamber, the fuel droplets are partially evaporated and then mixed with the oxidiser. The chemical reaction plays a key role in this period until the auto-ignition takes place. The remaining unmixed fuel is then burned more slowly due to limited oxidiser. Therefore, spray combustion can be considered as a partially premixed combustion mode. Thus, standard combustion models based on the fully premixed or fully non-premixed theories are not exactly appropriate for this concern.

Many studies have been performed to investigate the underlying physics governing partially premixed combustion [3–6]. These studies strived to capture spray combustion accurately and efficiently. In general, the key parameter used to predict the partially premixed lifted flames is the reaction progress variable. The method widely applied to model diffusion flame is the laminar flamelet approach proposed by Peters [7]. The formulations of the flamelet that incorporate the reaction progress variable are the steady flamelet model (SFM) and unsteady flamelet model (UFM).

The basic concept of the laminar flamelet model, as introduced by Peters [7], considers that the turbulent diffusion flames behave locally as an ensemble of laminar stretched flamelets. Each laminar flamelet is subjected to the local flow field, convecting and

* Corresponding author.
E-mail address: dhuchakallaya@yahoo.com (I. Dhuchakallaya).

1359-4311/$ – see front matter © 2013 Elsevier Ltd. All rights reserved.
http://dx.doi.org/10.1016/j.applthermaleng.2012.12.016

stretching in terms of the instantaneous scalar dissipation rate at the stoichiometric condition. This model is generally adopted based on a steady state assumption and thus, it is known as the steady flamelet model. The flame structure then can be described just by the local mixture fraction and the scalar dissipation rate as independent variables. Therefore, the thermochemical variables of flame field such as temperature, species mass fractions, density, etc., can be pre-calculated and tabulated into a database; the so-called flamelet library. This makes the SFM popular in turbulent combustion studies. This model has been successfully applied to turbulent combustion [8–10]. Subsequently, many theoretical and experimental studies [10–12] have identified the deficiency of the steady state assumption, in that the laminar flamelet structure cannot sufficiently respond to the rapid changes of scalar dissipation rate in the turbulent flow field. Due to a highly non-homogeneous and transient environment in the spray, the SFM is not able to predict the extinction and re-ignition of these flames. The incorrect lift-off of diffusion flames results in large discrepancies in flow field predictions, which would certainly yield inaccuracies in the prediction of pollutants [6]. In addition, the accuracy of this model decreases as the Damköhler number decreases [13]. The Damköhler number is characterised as the ratio of the turbulent to chemical time scales. When the chemistry is fast compared with the turbulent scale (large Damköhler number), the diffusion flame layer is supposed to be relatively thin. Because the Damköhler number is small, the local flame structure is then far from the assumption of a laminar flamelet.

The local extinction and re-ignition states cannot be described properly by SFM. The reason for this is that the solution space used in SFM is very restrictive. Typically, the ignition and extinction states are defined as the turning points on the S-curve, as shown in Fig. 1. The upper branch indicates the stable burning flames, and the lower branch is the non-reactive solutions. The middle branch is unstable solutions that are obtained from the flamelet equations. In SFM, only the upper and lower branches are used. Because the solutions need to jump between the upper turning point and the lower branch for dissipation rates around the extinction limit, the numerical solutions become unstable. In order to eliminate this weakness of SFM, a relevant time variable is introduced into the flamelet structures. This leads to the unsteady flamelet models. The importance of transient effects in flamelets models is described by Haworth et al. [14]. Many researchers have attempted to apply the unsteady flamelet model to combustion with local extinction and re-ignition. Mauss et al. [15] investigated the extinction and re-ignition of methane jet diffusion flames based on the unsteady flamelet model. Pitsch and Fedotov [16] developed a stochastic, interacting flamelet model, which extended the unsteady flamelet model to account for re-ignition effects due to the interaction of different flamelets. An application of the unsteady flamelet model to large eddy simulation was also demonstrated for a piloted jet diffusion flame by Pitsch and Steiner [17] and an excellent agreement with experimental data was obtained.

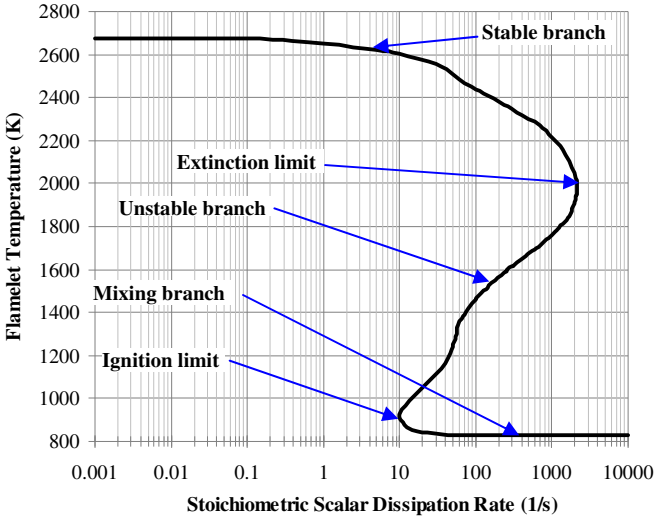

Fig. 1. Unsteady flamelet solution space for *n*-heptane/air flame.

To broaden the ability of the classical steady flamelet model in predicting the extinction and re-ignition of diffusion flames, Peters [4] introduced the reaction progress variable to SFM. Pierce and Moin [6] modified this approach by applying the reaction progress variable instead of the scalar dissipation rate to parameterise the flamelet library, in order to predict the local extinction and re-ignition of non-premixed turbulent combustion. Later, such a methodology was investigated and improved by Ihme and Pitsch [18,19]. Furthermore, the distribution of reaction progress variable with beta- and delta-probability density functions (PDF) for lifted flames in the Reynolds-averaged Navier–Stokes (RANS) and large eddy simulation (LES) frameworks was also studied by Ravikanti [3]. The lift-off length and temperature predictions are very encouraging. However, the presumed delta PDF presents an under-prediction of flame lift-off length. All the above investigations were conducted based on the consideration of a steady flamelet solution with reaction progress variable.

To improve the numerical accuracy, the unsteady flamelet solutions are used in combination with the reaction progress variable to predict the partially premixed flames. This approach was used with reasonable success by Pitsch and Ihme [20] in predicting emissions in non-premixed flames. With this confidence, the present study uses the unsteady flamelet approach with the variations in scalar dissipation rate, coupled with the reaction progress variable approach, to predict the lifted flames of diesel spray, which is considered as partially premixed flames. Certainly, the computational cost of the unsteady flamelet approach is marginally greater than the steady flamelet model. To reduce computational cost, the delta PDF for both the progress variable and scalar dissipation rate and the beta PDF for the mixture fraction, are presumed in this flamelet library. In addition, extensive experimental and numerical investigations [21–23] indicate that the delta PDF is a good approximation for the scalar dissipation rate. Hence, the objective of the present work is to capture efficiently the auto-ignition and flame lift-off for diesel spray flames by means of the unsteady/reaction progress variable combustion model in a RANS framework.

2. Unsteady/progress variable approach

The flamelet model introduced by Peters [4], assumes that the thin reacting layer embedded in a turbulent flow field is much smaller than the Kolmogorov length scale, the smallest length scale. The structure of this reaction zone then remains laminar and diffusive transport occurs in the direction normal to the surface of stoichiometric mixture. Under the unity Lewis number assumption, the one-dimensional flamelet equation can transform into the mixture mass fraction space, as follows:

$$\rho\frac{\partial Y_i}{\partial \tau}-\rho\frac{\chi}{2}\frac{\partial^2 Y_i}{\partial Z^2}=\dot{\omega}_i \tag{1}$$

and

$$\rho\frac{\partial T}{\partial \tau}-\rho\frac{\chi}{2}\left(\frac{\partial^2 T}{\partial Z^2}+\frac{1}{c_p}\frac{\partial c_p}{\partial Z}\frac{\partial T}{\partial Z}\right)=-\frac{1}{c_p}\sum_{i=1}^{N}h_i\dot{\omega}_i \tag{2}$$

where τ, c_p, Y_i, h_i and $\dot{\omega}_i$ are the time, specific heat at a constant pressure, mass fraction, enthalpy and chemical production rate of the ith species, respectively.

Generally, the distribution of the scalar dissipation rate χ in the Z space is presumed. The popular functional form of such a distribution in a counterflow diffusion flame is an inverse error function, as proposed by Peters [7]; however, other expressions have been proposed [24,25]. The inverse error function can be written as:

$$\chi(Z) = \frac{a_s}{\pi}\exp\left\{-2\left[erfc^{-1}(2Z)\right]^2\right\} \tag{3}$$

where a_s is the strain rate, indicating the maximum velocity gradient and $erfc^{-1}$ is the inverse error function. Eliminating the physical space parameter a_s, the scalar dissipation rate at stoichiometric condition is introduced. Thus, the distribution of χ as a function of Z can be rewritten as:

$$\chi(Z) = \chi_{st}\frac{\exp\left\{-2\left[erfc^{-1}(2Z)\right]^2\right\}}{\exp\left\{-2\left[erfc^{-1}(2Z_{st})\right]^2\right\}} \tag{4}$$

Thus, the solutions of flamelet equations can be written as $\phi(Z, \chi_{st})$, where ϕ denotes for species mass fractions, temperature or chemical source terms.

As shown in Fig. 2, the S-shaped curve of the unsteady flamelet solutions represents the stoichiometric temperature as the function of stoichiometric scalar dissipation rate. For a given scalar dissipation rate, there are multiple solutions of stoichiometric temperatures. Definitely, a new parameter has to be introduced to parameterise the unsteady flamelet solutions. This parameter, the so-called reaction progress variable C, identifies the unique state of each single flamelet along the S-shaped curve covering all the branches. The reaction progress variable is commonly defined as the summation of product mass in different ways [19,26–28]. In the present work, the definition of Ref. [19] is chosen as follows:

$$C = Y_{CO_2} + Y_{CO} + Y_{H_2O} + Y_{H_2} \tag{5}$$

For construction of the flamelet library, the reaction progress variable and scalar dissipation rate are independent parameters together with the mixture fraction. Therefore, each scalar dissipation rate has an individual distribution of reaction progress variable and mixture fraction. In Fig. 2, the vertical dots in the middle branch represent the individual unsteady flamelet solutions between the equilibrium and unburned limits. Thus, each flamelet solution depends on the mixture fraction Z, the reaction progress variable C and the stoichiometric scalar dissipation rate χ_{st}. The flamelet space for any scalar can be expressed as:

$$\phi = \phi(Z, C, \chi_{st}) \tag{6}$$

The reaction progress variable and scalar dissipation rate are independent of the mixture fraction. These three parameters are then assumed to be independent of each other and thus, the joint PDF is simplified as:

$$\tilde{P}(Z, C, \chi_{st}) = \tilde{P}(Z)\tilde{P}(C)\tilde{P}(\chi_{st}) \tag{7}$$

Here, the distribution of the mixture fraction is assumed to be beta-PDF and a delta-function closure for the reaction progress variable. The distribution of the scalar dissipation rate is assumed to follow a delta-PDF distribution. Hence, the above equation can be represented as:

$$\tilde{P}(Z, C, \chi_{st}) = \beta\left(Z; \tilde{Z}, \widetilde{Z''^2}\right)\delta\left(C; \tilde{C}\right)\delta\left(\chi_{st}; \widetilde{\chi_{st}}\right) \tag{8}$$

The mean scalars $\tilde{\phi}$ can be determined from the instantaneous flamelet solutions by weighting them with a joint PDF as:

$$\tilde{\phi} = \int_0^{\chi_q}\int_0^{C_{max}}\int_0^1 \phi(Z, C, \chi_{st})\tilde{P}\left(Z; \tilde{Z}, \widetilde{Z''^2}\right)\tilde{P}\left(C; \tilde{C}\right)\tilde{P}\left(\chi_{st}; \widetilde{\chi_{st}}\right)\mathrm{d}Z\mathrm{d}C\mathrm{d}\chi_{st} \tag{9}$$

where χ_q is the quenching strain rate. With this expression, a flamelet library of all mean scalars $\tilde{\phi}$ can be constructed as a function of the mean values of the mixture fraction $\tilde{Z}$, its variance $\widetilde{Z''^2}$, reaction progress variable $\tilde{C}$ and stoichiometric scalar dissipation rate $\widetilde{\chi_{st}}$.

The unsteady flamelet solutions employed here are solved by the FlameMaster code developed by Pitsch [29]. The skeletal mechanism for n-heptane with 43 species and 185 reactions of Liu et al. [30] is used. In Fig. 2, for a specific scalar dissipation rate, the initial conditions start from a non-burning flamelet. As the chemical reaction grows, the temperature continues to increase until ignition is reached at some mixture fraction. The development of the temperature profile then ends up at the steady flamelet solution. For n-heptane/air combustion, temperatures up to 2650 K are observed for small χ_{st} and the maximum temperature then drops beneath 2000 K at a value of about 2100 s^{-1} prior to extinction. As seen at $\chi_{st} = 100$ s^{-1}, the peaks of stoichiometric temperature

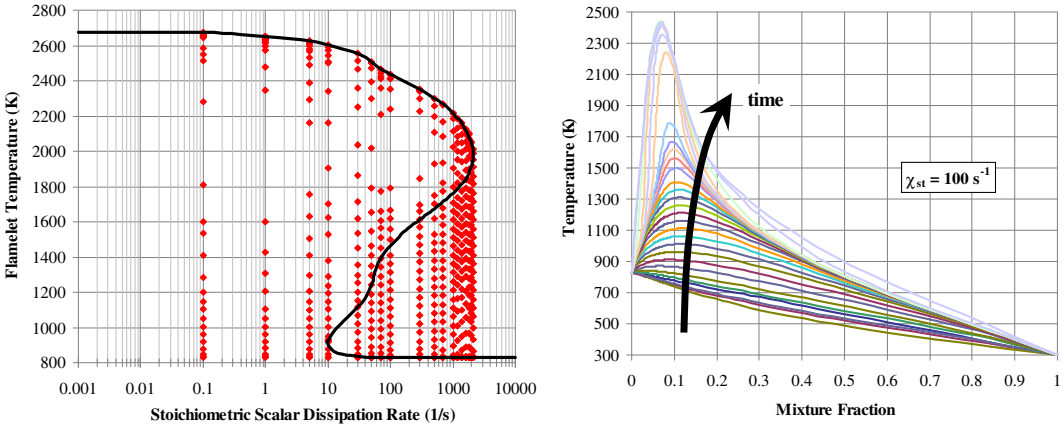

Fig. 2. S-shaped curve for n-heptane/air flame and temperature history at $\chi_{st} = 100$ s^{-1} ($T_f = 298$ K, $T_a = 830$ K, 27 bar).

slightly shift to lower values of mixture fraction with time. The development of the reaction progress variable distribution in the mixture fraction space for various scalar dissipation rates is also shown in Fig. 3. As the turbulent fluctuation becomes stronger (higher $\widetilde{\chi_{st}}$), the peaks of the reaction progress variable distribution profile (graph on the left) are definitely lower. This is because the turbulence significantly disturbs the chemical reactions resulting in a slower burning rate. Again, the time evolution of peaks for the reaction progress variable profile obviously shifts to lower values of mixture fraction. This represents a unique relationship among $\tilde{C}$, $\tilde{Z}$ and $\widetilde{\chi_{st}}$ to map a single thermochemical scalar in the unsteady flamelet approach.

As explained above, the mean thermochemical properties stored in the flamelet library are a function of $\tilde{Z}$, $\widetilde{Z''^2}$, $\tilde{C}$ and $\widetilde{\chi_{st}}$. These quantities can be determined from the transport equations for the reaction progress variable, mixture fraction and its variance. The transport equation for the Favre-averaged reaction progress variable, based on the assumption of unity Lewis number for all species involved, is given as:

$$\frac{\partial \overline{\rho}\tilde{C}}{\partial t}+\frac{\partial \overline{\rho}\tilde{U}_i\tilde{C}}{\partial x_i}=\frac{\partial}{\partial x_i}\left\{\left(\overline{\rho}D_C+\frac{\mu_t}{Sc_C}\right)\frac{\partial \tilde{C}}{\partial x_i}\right\}+\overline{\dot{\omega}}_C \tag{10}$$

where D is the diffusion coefficient and Sc is the Schmidt number. $\overline{\dot{\omega}}$ is the mean chemical source term of $\tilde{C}$. Referring to the definition of $\tilde{C}$, this source term is then defined as the summation of production rates of major combustion products:

$$\overline{\dot{\omega}}_C=\overline{\dot{\omega}}_{CO_2}+\overline{\dot{\omega}}_{CO}+\overline{\dot{\omega}}_{H_2O}+\overline{\dot{\omega}}_{H_2} \tag{11}$$

For spray combustion, the mixture fraction is no longer a conserved scalar because of the evaporation of spray droplets [31,32]. In order to take into account the evaporation effect, the transport equation for mixture fraction is modified as:

$$\frac{\partial \overline{\rho}\tilde{Z}}{\partial t}+\frac{\partial \overline{\rho}\tilde{U}_i\tilde{Z}}{\partial x_i}=\frac{\partial}{\partial x_i}\left\{\left(\overline{\rho}D_Z+\frac{\mu_t}{Sc_Z}\right)\frac{\partial \tilde{Z}}{\partial x_i}\right\}+S_m \tag{12}$$

where S_m is the mass transfer rate due to the evaporation of the liquid droplets. The mixture fraction is defined by Bilger [33] as:

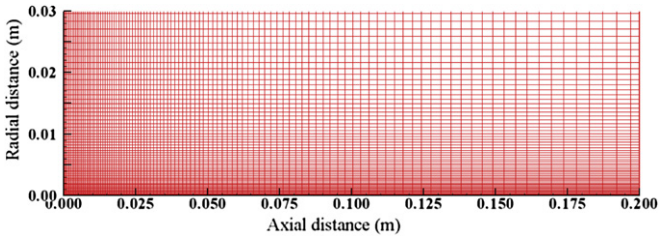

Fig. 4. Grid used in the spray combustion (The domain is 0.2 m long and 0.03 m in radius with 109 × 73 cells).

$$Z=\frac{2\frac{Y_C-Y_{C,2}}{M_C}+\frac{1}{2}\frac{Y_H-Y_{H,2}}{M_H}-\frac{Y_O-Y_{O,2}}{M_O}}{2\frac{Y_{C,1}-Y_{C,2}}{M_C}+\frac{1}{2}\frac{Y_{H,1}-Y_{H,2}}{M_H}-\frac{Y_{O,1}-Y_{O,2}}{M_O}} \tag{13}$$

where M is the molecular mass and the subscripts C, H and O indicate the quantities for the elements carbon, hydrogen and oxygen, respectively. The subscripts 1 and 2 refer to the constant mass fraction in the original fuel and oxidiser streams, respectively.

The mixture fraction variance is also needed when the probability density function must be evaluated. The Favre-averaged balance equation of the mixture fraction variance can be written as:

$$\frac{\partial \overline{\rho}\widetilde{Z''^2}}{\partial t}+\frac{\partial \overline{\rho}\tilde{U}_i\widetilde{Z''^2}}{\partial x_i}=\frac{\partial}{\partial x_i}\left\{\left(\overline{\rho}D_{\widetilde{Z''^2}}+\frac{\mu_t}{Sc_{\widetilde{Z''^2}}}\right)\frac{\partial \widetilde{Z''^2}}{\partial x_i}\right\}+2\frac{\mu_t}{Sc_{\widetilde{Z''^2}}}\left(\frac{\partial \tilde{Z}}{\partial x_i}\right)^2-\overline{\rho}C_\chi\frac{\tilde{\varepsilon}}{\tilde{k}}\widetilde{Z''^2} \tag{14}$$

where C_χ is about 2.0.

3. Numerical method and validated configuration

In this study, the main effort focuses on the application of spray on combustion phenomena. In order to simplify, the uncomplicated geometry of the combustion chamber, as studied here, is axisymmetric, as shown in Fig. 4. The Favre-averaged Navier–Stokes approach is sufficiently appropriate to lead to a successful study on the turbulence–chemistry interaction. Based on the finite

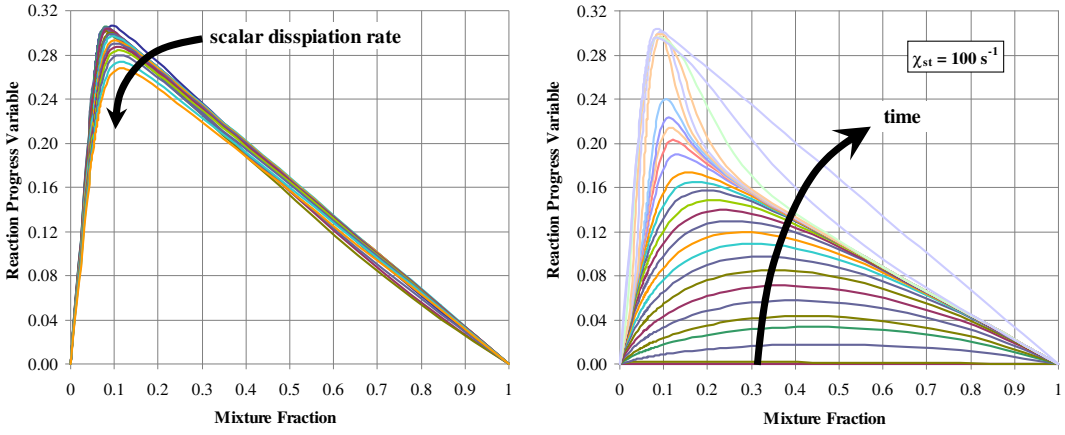

Fig. 3. Reaction progress variable distribution for various scalar dissipation rates and its development.

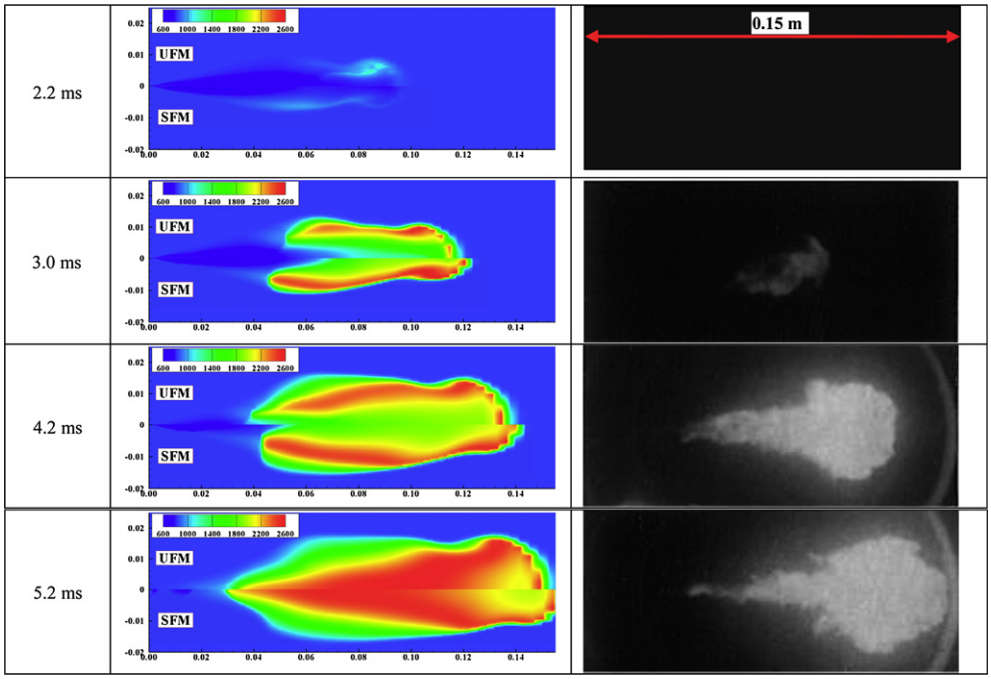

Fig. 5. Comparison between predicted flame temperature distributions and photographs of flame luminosity [2].

volume method, the solution of the transport equation system is carried out in an Eulerian framework. All the conservation or transport equations for both the liquid and gas phases are solved on the same two-dimensional (z, r) axisymmetric orthogonal computational grid. A staggered grid arrangement is adopted for the liquid and gas phase velocity components. Euler implicit temporal differencing and hybrid upwind/central spatial differencing are employed to render all the liquid and gas phase transport equations into a finite volume framework. The sub-models for droplet breakup, collision, evaporation and the interactions between the liquid phase and gas phase, are detailed in Beck and Watkins [34], based on the drop number size moment scheme. In high Reynolds number spray combustion, a standard k–ε turbulent model can perform efficiently due to low computational cost. The wall function of Launder and Spalding [35] is taken into account for the effects of a near wall flow. The solution algorithm is based on the PISO algorithm of Issa [36], with the liquid phase equations added to it. The accuracy of such an approach has been partially assessed in earlier publications [34,37–43], both in non-reactive and reactive applications. Numerous grid and time-step dependence tests have also been carried out in the earlier publications. The results from those tests have been used to set these parameters in this work.

In the flamelet library generated in this work, the mixture fraction and its variance spaces are divided into 141 and 21 cells, respectively. A set of 18 flamelets is created with the stoichiometric dissipation rate ranging from 0.1 to 2125.13 and the corresponding extinction limit $\chi_{st,\,q}$ is found to be about 2125.13 s^{-1}. In every single dissipation rate step, the reaction progress variable space is subdivided into 29 flamelets. Hence, the thermochemical properties can be recalled by mapping these flamelets within their validity ranges.

The experimental investigation used for validation of this simulation model is the diesel spray combustion measurements of Akiyama et al. [2]. A 0.18-mm-diameter nozzle is used to inject the

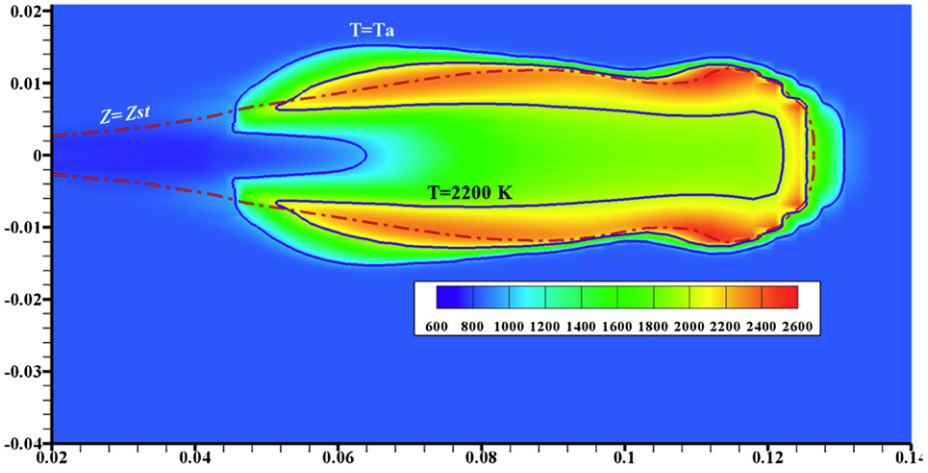

Fig. 6. Lifted flame temperature contour predicted by unsteady flamelet model.

diesel liquid with a maximum pressure of 80 MPa. The air in the combustion chamber is preheated to 830 K and pressurised to 27 bar. The quantity of liquid diesel injected is 28 mg during the 3.8 ms of the injection period. The ignition delay time is evaluated by the combustion chamber pressure history and the flame temperature is analysed by the two-colour method. A spray distribution with a Sauter Mean Radius of 10 microns is presumed in this simulation and the time-step in the calculation is 0.5 μs.

4. Results and discussion

The temperature evolution from the early stage of ignition to further combustion of the spray, compared with the experimental results of Akiyama et al. [2], is shown in Fig. 5. The upper and lower halves of the plots represent the flame temperature contours predicted by the unsteady and steady flamelet models combined with the reaction progress variable, respectively. In the SFM, the mean chemical source term of reaction progress variable in Eq. (10) is obtained by the PDF–EBU scheme proposed by Dhuchakallaya and Watkins [43]. This source term is a combination of a single-step chemical reaction rate and Eddy break-up model. In Fig. 5, the reactive activity begins at the outer edge of the spray, as shown by means of a locally increased temperature. The ignition kernel of SFM in particular, occurs close to the place where the flame lift-off will settle, whereas this activity is placed further downstream in the UFM. Both models are satisfactory in predicting the ignition delay time at approximately 2.2 ms; however, the first appearance of the significant luminous flame in the experiment is observed later, at around 2.8 ms. The flame then propagates downstream and upstream from the ignition locations. The outer edge of the spray is consequently fully reacted and the combustion region expands to the inner volume and the maximum temperature continues to rise. As seen, the SFM presents a slightly larger high-temperature region than the UFM. In the present work, the flame lift-off length is defined as the height from the nozzle tip to the threshold temperature. Because there is no certain threshold temperature to define the lift-off length in the simulation, the threshold temperature of 2200 K is chosen, as in Refs. [44,45]. The lift-off lengths obtained from both models are relatively comparable at about 50 mm, as the lift-off length measured directly from photographs is around 48 mm. This length corresponds to the approximated power-law scaling of Siebers et al. [46], which gives this value in the range of 40–55 mm. The flame shapes obtained from the UFM are more closely related to the luminous flames than those predicted by SFM, especially in the spray head region.

The lifted flame is represented by the temperature contour, as shown in Fig. 6, taken at the time of 3.7 ms after injection. In the inner region of the spray downstream of the lift-off, the temperature gradually increases due to the partially premixed rich flame. It is clearly shown that higher temperatures appear over the stoichiometric contour, as expected in diffusion flames. The flame lift-off predicted by the unsteady flamelet model is around 51 mm. From this figure, it can be stated that the present model is able to capture, at least qualitatively, the main features of the diesel flame structure.

The predicted flames clearly emerge prior to the flame luminosity, as seen in Fig. 7 and then the discrepancy of the predicted flame areas with the experimental results trends towards stable values. This illustrates that both models give over-predictions of flame propagation. However, the flame area found in the UFM is obviously closer to the experimental results than the SFM prediction. This might be because the source term of reaction progress variable employed in the SFM is based on a chemical time scale that is derived from a single-step irreversible chemical reaction. This naturally provides an over-prediction in reaction rate, as has been

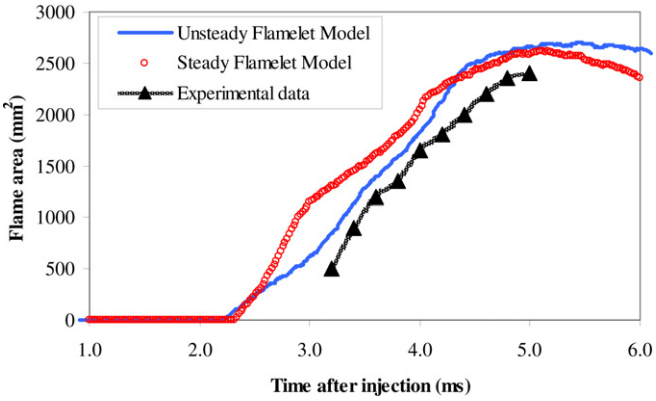

Fig. 7. Development of flame area compared with the experimental results of Akiyama et al. [2].

reported by many researchers. This is also shown in Fig. 5, where the thicker band of high temperature appears in the SFM prediction. As observed in the experiment, the flame front approaches the combustion chamber wall at the time of 5.2 ms. Therefore, the results after the time of 5.2 ms are not considered.

As shown in Fig. 8, the heat release rate in the early stages slightly decreases below zero due to the heating of the liquid droplets. It then increases sharply after ignition leading to the peak reaction rate. Consequently, the shortage of mixing improperly between fuel vapour and air becomes dominant, resulting in the diffusion flame behaviour revealed later on. As shown in the comparison, the SFM prediction apparently correlates well with the experimental data in the early stages of combustion. This is certainly due to the fine-tuning of the modelling constants of $\overline{\omega}_C$ in the PDF–EBU approach, which depends on both the structure of the flame and the chemical reaction. This differs appreciably from the UFM scheme where $\overline{\omega}_C$ is taken from the flamelet database, which requires no further tuning. The peak of experimental results is significantly lower than that predicted by both models. However, in the main combustion, both models function very similarly to the experimental data. Interestingly, a large discrepancy emerges beyond 4.8 ms after injection. This might be due to the disturbance of the wall, which the flame front impacts at a time of 5.2 ms. In all aspects of comparison, the UFM is apparently better able to match the experimental results than the SFM prediction.

The distribution of flame temperature in the mixture fraction space is represented as scatter plots shown in Fig. 9. During the

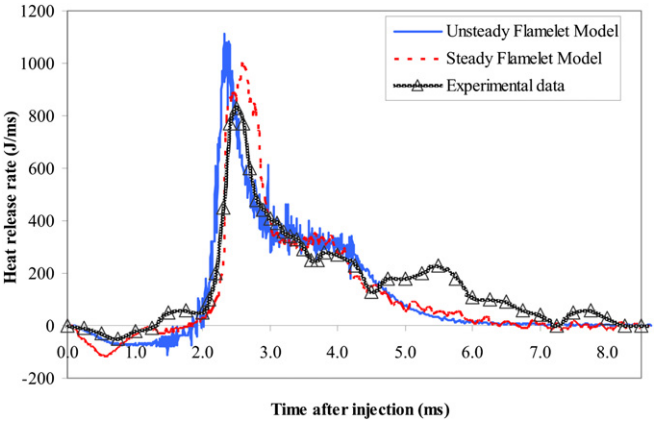

Fig. 8. Time history of heat release rates compared with the measurements of Akiyama et al. [2].

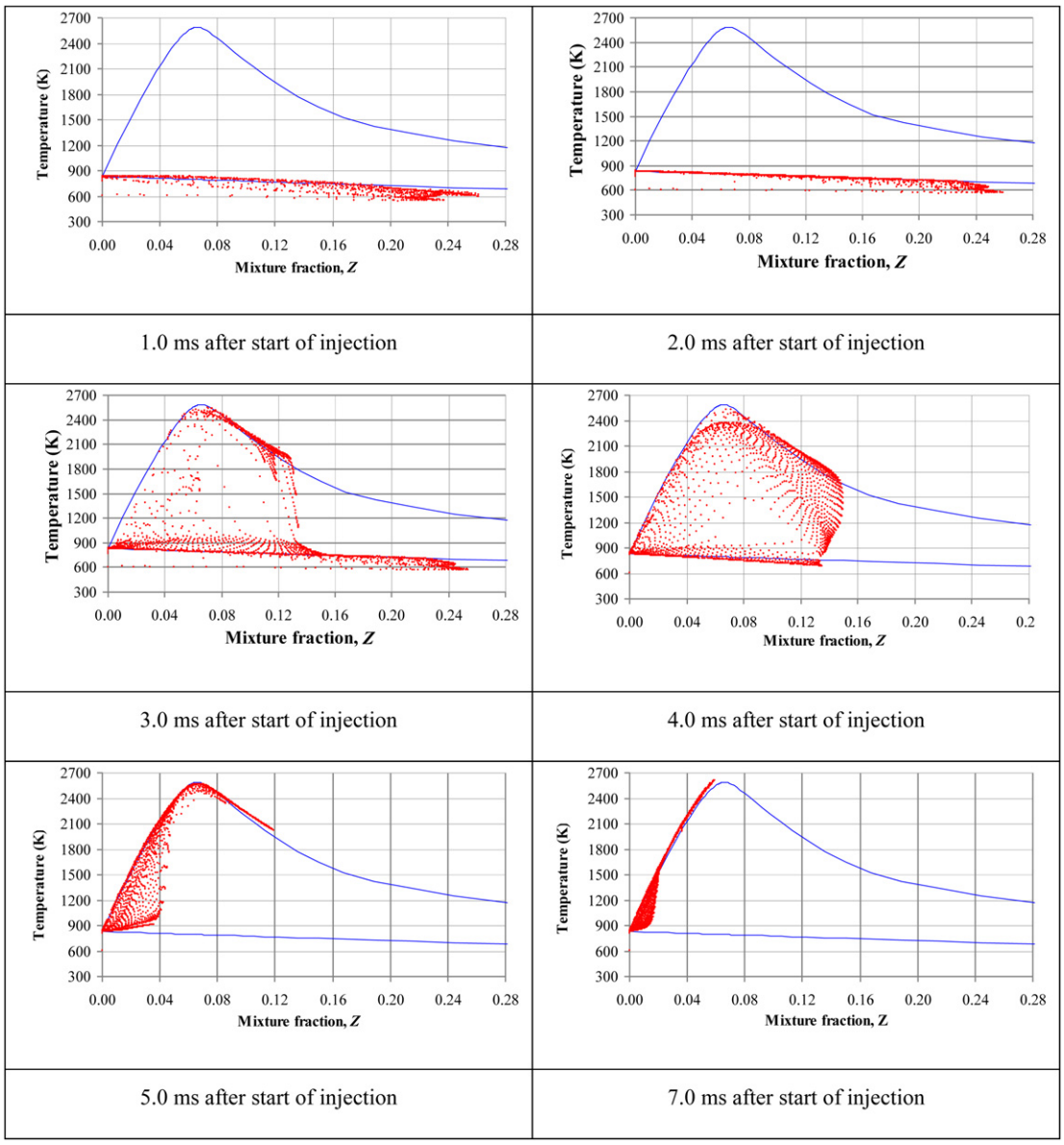

Fig. 9. Scatter plot of predicted temperature in Z space during combustion (blue lines denote to equilibrium states). (For interpretation of the references to colour in this figure legend, the reader is referred to the web version of this article.)

heating period in the first 2 ms, all temperature data are close to the mixing limit. Some are located beneath this line due to the evaporating cooling of spray droplets. Auto-ignition takes place at a time of 2.2 ms and the temperature then starts rising to continue the main combustion process later on. The predicted temperatures vary between the mixing and equilibrium states, because the lifted flame tries to detach and re-ignite in the period of 3 and 4 ms. Following the end of injection at 3.8 ms, the data begin to depart from the mixing to equilibrium lines. As the spray combustion process continues, the temperatures rise increasingly close to the equilibrium state. Hence, the lifted flame is well represented by this developed model.

5. Conclusions

In the present study, the unsteady flamelet model, combined with the reaction progress variable approach, is implemented to describe and analyse auto-ignition and combustion phenomena in a turbulent environment for conditions typically encountered in internal combustion engines. The spray model employed is based on the droplet size distribution moments approach introduced by Beck [1]. This simulation study with *n*-heptane as a surrogate for diesel fuel, demonstrates the model's capabilities to capture the spray formation, subsequent auto-ignition and the existence of a lift-off length. The results show that this approach appears to be an effective method for capturing essential flame characteristics, such as auto-ignition and flame lift-off, without the need to apply any additional ignition model, as compared with the experimental results of Akiyama et al. [2]. The predicted flame temperature contours are reasonably comparable to the formations of luminous flames. However, the UFM provides a small over-prediction in flame area but overall, the UFM performs slightly better than the SFM. Therefore, the unsteady flamelet/reaction progress variable model can be applied with confidence for partially premixed lifted flames, such as diesel spray in reciprocating engines.

References

[1] J.C. Beck, Computational modelling of polydisperse sprays without segregation into droplet size Classes, Ph.D. thesis, UMIST, Manchester, (2000).
[2] H. Akiyama, H. Nishimura, Y. Ibaraki, N. Iida, Study of Diesel Spray Combustion and Ignition Using High-pressure Fuel Injection and a Micro-hole Nozzle with a Rapid Compression Machine: Improvement of Combustion Using Low Cetane Number Fuel, vol. 19, Society of Automotive Engineers of Japan, 1998, pp. 319–327.
[3] V.V.S.M. Ravikanti, Advanced Flamelet Modeling of Turbulent Non-premixed and Partially Premixed Combustion, Loughborough University, UK, 2008.
[4] N. Peters, Turbulent burning velocity for large-scale and small-scale turbulence, Journal of Fluid Mechanics 384 (1999) 107–132.
[5] H. Pitsch, Unsteady flamelet modeling of differential diffusion in turbulent jet diffusion flames, Combustion and Flame 123 (2000) 358–374.
[6] C.D. Pierce, P. Moin, Progress-variable approach for large eddy simulation of non-premixed turbulent combustion, Journal of Fluid Mechanics 504 (2004) 73–97.
[7] N. Peters, Laminar diffusion flamelet models in non-premixed combustion, Progress in Energy and Combustion Science 10 (1984) 319–339.
[8] M. Hossain, CFD Modeling of Turbulent Non-premixed Combustion, Loughborough University, UK, 1999.
[9] C. Hollmann, E. Gutheil, Flamelet-modeling of turbulent spray diffusion flames based on a laminar spray flame library, Combustion Science and Technology 135 (1998) 175–192.
[10] J.C. Ferreira, Steady and transient flamelet modelling of turbulent non-premixed combustion, Progress in Computational Fluid Dynamics 1 (2001) 29–42.
[11] F.N. Egolfopoulos, C.S. Campbell, Unsteady counterflowing strained diffusion flames: diffusion-limited frequency response, Journal of Fluid Mechanics 318 (1995) 1–29.
[12] J. Park, H.D. Shin, Experimental investigation of the developing process of an unsteady diffusion flame, Combustion and Flame 110 (1997) 67–77.
[13] A.W. Cook, J.J. Riley, G. Kosaly, A laminar flamelet approach to subgrid-scale chemistry in turbulent flows, Combustion and Flame 109 (1997) 332–341.
[14] D.C. Haworth, M.C. Drake, R.J. Blint, Stretched laminar flamelet modeling of a turbulent jet diffusion flame, Combustion Science and Technology 60 (1988) 287–318.
[15] F. Mauss, D. Keller, N. Peters, A Lagrangian simulation of flamelet extinction and re-ignition in turbulent jet diffusion flames, in: Symposium (International) on Combustion, vol. 23, 1991, pp. 693–698.
[16] H. Pitsch, S. Fedotov, Investigation of scalar dissipation rate fluctuations in non-premixed turbulent combustion using a stochastic approach, Combustion Theory and Modelling 5 (2001) 41–57.
[17] H. Pitsch, H. Steiner, Large-eddy simulation of a turbulent piloted methane/air diffusion flame (Sandia flame D), Physics of Fluids 12 (2000) 2541–2554.
[18] M. Ihme, H. Pitsch, Prediction of extinction and reignition in nonpremixed turbulent flames using a flamelet/progress variable model 1; a priori study and presumed PDF closure, Combustion and Flame 155 (2008) 70–89.
[19] M. Ihme, H. Pitsch, Prediction of extinction and reignition in nonpremixed turbulent flames using a flamelet/progress variable model 2; application in LES of Sandia flames D and E, Combustion and Flame 155 (2008) 90–107.
[20] H. Pitsch, M. Ihme. An unsteady/flamelet progress variable method for LES of nonpremixed turbulent combustion, in: AIAA Paper 2004-557. 2005.
[21] L.K. Su, N.T. Clements, Planar measurements of the full three-dimensional scalar dissipation rate in gas-phase turbulent flows, Experiments in Fluids 27 (1999) 507–521.
[22] H. Pitsch, H. Steiner, Scalar mixing and dissipation rate in large-eddy simulations of non-premixed turbulent combustion, in: Proceedings of the 28th International Symposium on Combustion, The Combustion Institute, Pittsburg, 2000.
[23] V. Eswaran, S.B. Pope, Direct numerical simulations of the turbulent mixing of a passive scalar, Physics of Fluids 31 (1988) 506–520.
[24] J.S. Kim, A. Williams, Structures of flow and mixture fraction fields for counterflow diffusion flames with small stoichiometric mixture fractions, SIAM Journal on Applied Mathematics 53 (1993) 1551–1566.
[25] H. Pitsch, M. Chen, N. Peters, Unsteady flamelet modeling of turbulent hydrogen/air diffusion flames, Proceedings of the Combustion Institute 27 (1998) 1057–1064.
[26] C. Bekdemir, Numerical Modeling of Diesel Spray Formation and Combustion, Eindhoven University of Technology, Netherlands, 2008.
[27] Y. Baba, R. Kurose, Analysis and flamelet modelling for spray combustion, Journal of Fluid Mechanics 612 (2008) 45–79.
[28] S.K. Sadasivuni, W. Malalasekera, S.S. Ibrahim. Validation of unsteady flamelet/progress variable methodology for non-premixed turbulent partially premixed flames, in: Proceedings of the ECM 2009 Fourth European Combustion Meeting, Vienna University of Technology, Austria. 2009.
[29] H. Pitsch, in: A C++ Computer Program for 0-D and 1-D Laminar Flame Calculations, RWTH Aachen, 1988.
[30] S. Liu, J.C. Hewson, J.H. Chen, H. Pitsch, Effects of strain rate on high-pressure nonpremixed *n*-heptane autoignition in counterflow, Combustion and Flame 137 (2004) 320–339.
[31] H. Watanabe, R. Kurose, S. Hwang, F. Akamatsu, Characteristics of flamelet in spray flames formed in a laminar counterflow, Combustion and Flame 148 (2007) 234–248.
[32] H. Watanabe, R. Kurose, S. Komori, H. Pitsch, Effects of radiation on spray flame characteristics and soot formation, Combustion and Flame 152 (2008) 2–13.
[33] R.W. Bilger, S.H. Stårner, R.J. Kee, On reduced mechanisms for methane–air combustion in nonpremixed flames, Combustion and Flame 80 (1990) 135–149.
[34] J.C. Beck, A.P. Watkins, On the development of spray sub-models based on droplet size moments, Journal of Computational Physics 182 (2002) 586–621.
[35] B.E. Launder, D.B. Spalding, Lectures in Mathematical Models of Turbulence, Academic Press, London, 1972.
[36] R.I. Issa, Solution of the implicitly discretised fluid flow equations by operator-splitting, Journal of Computational Physics 62 (1986) 40–65.
[37] J.C. Beck, A.P. Watkins, The simulation of water and other non-fuel sprays using a new spray model, Atomization and Sprays 13 (2003) 1–26.
[38] J.C. Beck, A.P. Watkins, On the development of a spray model based on drop-size moments, Proceedings of the Royal Society of London – Series A 459 (2003) 1365–1394.
[39] J.C. Beck, A.P. Watkins, The droplet number moments approach to spray modelling: the development of heat and mass transfer sub-models, International Journal of Heat and Fluid Flow 2 (2003) 242–259.
[40] J.C. Beck, A.P. Watkins, The simulation of fuel sprays using the moments of the drop number size distribution, International Journal of Engine Research 5 (2004) 1–21.
[41] A.P. Watkins, Modelling of mean temperatures used for calculating heat and mass transfer in sprays, International Journal of Heat and Fluid Flow 28 (2007) 388–406.
[42] I. Dhuchakallaya, A.P. Watkins, Application of spray combustion simulation in DI diesel engine, Applied Energy 87 (2010) 1427–1432.
[43] I. Dhuchakallaya, A.P. Watkins, Numerical modelling of diesel spray auto-ignition and combustion, International Journal of Engine Research 12 (2011) 169–180.
[44] F.A. Tap, D. Veynante, Simulation of flame lift-off on a diesel jet using a generalized flame surface density modeling approach, Proceedings of the Combustion Institute 30 (2005) 919–926.
[45] P.K. Senecal, E. Pomraning, K.J. Richards, T.E. Briggs, C.Y. Choi, R.M. McDavid, M.A. Patterson. Multi-dimensional modeling of direct-injection diesel spray liquid length and flame lift-off using CFD and parallel detailed chemistry, in: SAE Technical Paper Series No. 2003-01-1043. 2003.
[46] D.L. Siebers, B.S. Higgins, L.M. Pickett. Flame lift-off on direct injection diesel fuel jets: oxygen concentration effects, in: SAE Technical Paper Series No. 2002-01-0890. 2002.